

## PROPAGATION ALONG SINGLE-CRYSTALLINE SILVER FILAMENTS WITH PEARL-CHAIN-LIKE STRUCTURES <sup>†</sup>

Z. Wu, B. Q. Zeng, and J. F. Zhu

National Laboratory for Vacuum Electronics  
School of Physical electronics  
University of Electronic Science & Technology of China  
Chengdu 610054, China

**Abstract**—Single-crystalline silver filaments with periodic pearl-chain-like structures are fabricated by electrodeposition without using any templates, surfactants, and additives. Simulations demonstrate that excited surface waves may sustain on silver pearl chains in middle infrared (Mid-IR) range. The propagation features of surface waves on the silver filaments indicate the structure application for Mid-IR wave transmittance.

### 1. INTRODUCTION

Both energy and information can be transmitted by waveguides made of metallic or dielectric materials at specific frequencies of electromagnetic waves. Optical fibers can be applied to confine and transfer light signals, while coaxial cables work well at microwave frequencies [1–3]. However, neither approach is efficient in transmission at infrared and terahertz bands. Recently, a waveguide based on coupled surface plasmon polaritons (SPPs) among aligned metallic dots has been realized in the optical range [4–6]. It has also been discovered that terahertz waves can be efficiently transferred along a corrugated metallic wire in the mode of spoof SPPs or mimicking SPPs [7, 8]. Highly localized SPPs can be sustained in the terahertz region. In this case, the dispersion and mode profile of the transmitted electromagnetic waves are determined by the geometry of the corrugation on metallic structures [8–10]. It opens the way for important applications such as energy concentration on cylindrical

---

*Received 12 June 2010, Accepted 22 July 2010, Scheduled 25 August 2010*

<sup>†</sup> Corresponding author: Z. Wu (wumingy1981@gmail.com).

wires and super-focusing using conical structures. However, there are two technical challenges which hinder rapid developments on the above design. First, in order to realize periodic corrugated structures on a metallic wire, microlithography techniques should be applied, which are usually time consuming and expensive. Second, single-crystalline metallic materials are preferred to reduce energy loss or signal noises, which are not easy to be fabricated due to the material anisotropy.

In this paper, we report the single-crystalline silver filaments with periodic, pearl-chain-like structures fabricated by electrodeposition. Simulations demonstrate that SPP-like surface waves may sustain on surface of the silver filaments in a wide region of middle-infrared (Mid-IR). It implies that such kind of metallic structures can serve in electromagnetic wave transmission, which may have applications for Mid-IR transmission or detection [11, 12].

## 2. EXPERIMENTS

An electrodeposition system [13–17] is exploited to fabricate microstructure single-crystalline silver filaments without using any templates, surfactants, and additives. The experimental details are analogous to previous works [13–17].  $\text{AgNO}_3$  aqueous electrolyte is prepared by dissolving  $\text{AgNO}_3$  (analytically pure, 99.8%) with de-ionized ultrapure water (Millipore, electric resistivity of  $18.2 \text{ M}\Omega\cdot\text{cm}$ ) and the concentration is 0.05 M. Parallel, straight electrodes are made of pure silver wires (99.99% pure, 0.5 mm in diameter, Goodfellow), and sandwiched by two glass slides. The separation between the silver electrodes is 10 mm. The temperature in the electrodeposition cell is decreased to  $-4^\circ\text{C}$  by a programmable thermostat (Polystat 12108-35, Cole-Parmer). A flat interface between ice and electrolyte is achieved with repeated solidification and melting method. Eventually a homogeneous, ultrathin layer of concentrated electrolyte of  $\text{AgNO}_3$  can be generated. In the electrodeposition, potentiostatic method is applied and the electric voltage is set to 0.3 V. The morphology of the electrodeposited silver filaments is characterized by a field emission scanning electron microscope (FESEM) (LEO-1530VP).

## 3. RESULTS & DISCUSSIONS

Electrodeposited silver filaments are silvery shiny in color and consist of pearl-chain-like structures. As shown in Fig. 1(a), silver filaments are ramified yet the periodic features on the filaments are evident. The average diameter of silver ‘pearl’ is around  $2 \mu\text{m}$ , which can be tuned by the initial electrolyte concentration of  $\text{AgNO}_3$  and the applied voltage

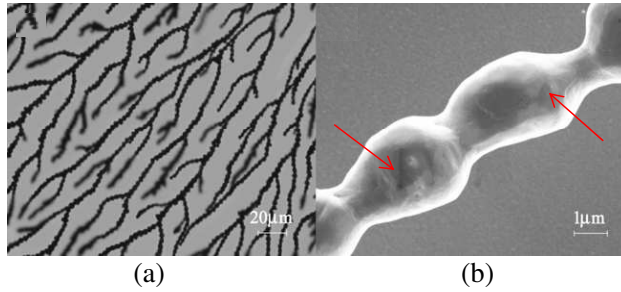


**Figure 1.** Morphology of electrodeposited silver filaments with pearl-chain-like structures. (a) Optical micrograph, (b) FESEM micrograph.

in the potentiostatic electrodeposition. Because of the coarseness in electrolyte [18, 19], silver ‘pearl’ presents round morphology. As arrows marked in the higher magnification of Fig. 1(b), there are some facets existing on the surface of silver pearls. It implies that this silver filament with pearl-chain-like structures is single-crystalline.

Silver filaments electrodeposited on glass substrate are sputtered with gold and pretreated with Focus Ion Beam (FIB) milling process. The FIB-milled silver filaments are observed with FESEM as shown in Fig. 2, where some compact and flat cutting surfaces can be identified. These silver filaments with pearl-chain-like structures have been demonstrated to be single-crystalline by the electron back scattering diffraction (EBSD) results in the previous work [17]. The exposed flat surfaces in Fig. 2 are mainly  $\{001\}$  facet and the growing direction of these silver filaments should be  $\langle 101 \rangle$ . In electrodeposition process, all silver filaments grow from an initial point on cathode and they are electrically connected. Branches are inevitable which may increase capacity and lead in energy loss in circuits. When the electromagnetic wave propagates along metallic filaments, scattering is evident at positions where branching occurs. Previous works have demonstrated that ramification of Cu filaments can be greatly reduced with the unique electrodeposition method [13, 14, 16]. Comparing to silver dendrites [20] and silver fractal structures [21], ramification of these silver filaments with pearl-chain-like structures is also greatly reduced with this unique electrodeposition method [17]. As illustrated in Fig. 2(b), the cross section of a silver Y-branch with pearl-chain-like structures is also compact and single-crystalline. This kind of Y-branches may have applications in electromagnetic devices, such as splitters [22–24].

The propagation along silver-pearl-chain arrays can be obtained by Fourier transform infrared (FT-IR) spectrometer associated with

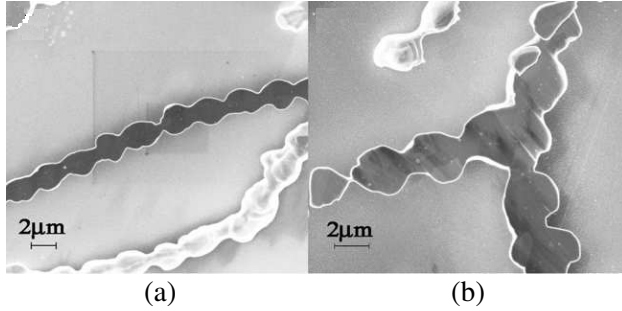


**Figure 2.** The cross sections of FESEM micrograph. (a) Straight silver filament with pearl-chain-like structures, (b) silver Y-branch with pearl-chain-like structures. Black regions are pretreated with FIB milling process and identify compact and flat cutting surfaces.

an infrared microscope with FPA detector [17]. In the measurement, the horizontal component of infrared light plays the role to excite resonance of SPPs on silver filaments. In the simulation, a periodical silver spherical chain is taken as the model. The diameter of each silver sphere and the period of silver spherical chain are  $2\ \mu\text{m}$  and  $1.8\ \mu\text{m}$ , respectively.  $N$  represents the number of silver spheres in the model. The propagation along an individual silver spherical chain and electric field distribution are simulated based on finite difference time-domain (FDTD) method. Electromagnetic wave is incident from one side of the silver spherical chain, and signals are received in the other side.

In the simulation, transmittance is defined as  $E_t/E_i$ , where  $E_i$  is the input electric field, and  $E_t$  is the electric field received in the other side of the silver spherical chain. Fig. 3 is the relative transmittance through a silver spherical chain with respect to vacuum, which presents the infrared propagated character of this silver spherical chain. As illustrated in Fig. 3, these transmitted spectra with different sphere number  $N$  have similar tendency. It is obvious that all these spectra can be divided into three parts. First, in the wave number region lower than  $800\ \text{cm}^{-1}$ , the transmittance is a little less than that in vacuum. Second, in the wave number region higher than  $2200\ \text{cm}^{-1}$ , the transmittance falls down rapidly and approaches zero. Third, in the wave number region between  $800\ \text{cm}^{-1}$  and  $2200\ \text{cm}^{-1}$ , transmission enhancement can be identified. In Fig. 3, as the sphere number  $N$  increases, the relative transmittance intensity with respect to vacuum and the peaks' number in these curves are all increased.

As illustrated in Fig. 3, wave numbers of  $1818\ \text{cm}^{-1}$ ,  $2222\ \text{cm}^{-1}$  and  $3030\ \text{cm}^{-1}$  are marked in the curve of  $N = 10$ . Wave numbers

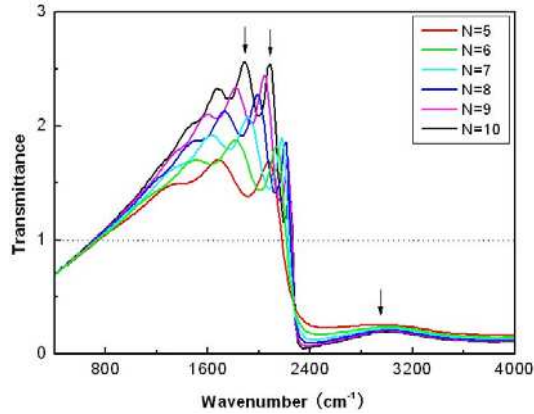


**Figure 3.** Relative transmittance through silver pearl chains with respect to vacuum. The number of silver spheres  $N = 5, 6, 7, 8, 9, 10$ . The arrows in the curve of  $N = 10$  are wave numbers of  $1818\text{ cm}^{-1}$ ,  $2222\text{ cm}^{-1}$  and  $3030\text{ cm}^{-1}$ , respectively.

$1818\text{ cm}^{-1}$  and  $2222\text{ cm}^{-1}$  correspond to two individual peaks in the transmission enhancement region. However, at  $3030\text{ cm}^{-1}$ , the relative transmittance approaches zero. Fig. 4 plots the electric field distribution on the cross section along silver spherical chain axis at wave numbers of  $1818\text{ cm}^{-1}$ ,  $2222\text{ cm}^{-1}$  and  $3030\text{ cm}^{-1}$ , respectively. At  $1818\text{ cm}^{-1}$ , electromagnetic wave can propagate along silver spherical chain, and strong electric field appears around the silver spherical chain as shown in Fig. 4(a). At  $2222\text{ cm}^{-1}$ , electromagnetic wave can also propagate along silver spherical chain, and the strong electric field appears around the silver spherical chain as shown in Fig. 4(b). It is observed that the propagating wavelength near silver spherical chain is longer in Fig. 4(a) than that in Fig. 4(b). As a result, electric field is mainly localized between a pair of silver spheres at  $1818\text{ cm}^{-1}$  in Fig. 4(a), while electric field is mainly localized around each silver sphere at  $2222\text{ cm}^{-1}$  in Fig. 4(b). However, at  $3030\text{ cm}^{-1}$  shown in Fig. 4(c), electromagnetic wave cannot propagate along this silver spherical chain and electric field is scattered at the incident site of this silver spherical chain. Almost no signals can be received in the other side. The simulated electric field distribution of Fig. 4 is in accordance with the relative transmittance spectra of Fig. 3.

When the periodically corrugated silver spherical chain is excited by the horizontal component of the incident infrared wave, an asymptotic frequency [8] is strongly depends on the geometrical structure of this silver spherical chain. According to Ref. [8], the

asymptotic frequency should be around  $2300\text{ cm}^{-1}$  for these silver pearl-chain-like structures. For incident frequency lower than the asymptotic frequency, spoof SPP can sustain on the surface of silver spherical chain. Electromagnetic wave can propagate along silver spherical chain as shown in Fig. 4(a) and Fig. 4(b). However, for incident frequency higher than the asymptotic frequency, spoof SPP cannot sustain on the surface of silver spherical chain. As a result, electromagnetic wave cannot propagate through the silver spherical chain and electromagnetic wave is scattered at the incident site as shown in Fig. 4(c).

Above results demonstrate that spoof SPP may sustain on the surface of corrugated silver pearls, and electromagnetic waves can propagate along these electrodeposited silver filaments with pearl-chain-like structures in a wide range of infrared. As these silver filaments with pearl-chain-like structures are self-assembled by electrodeposition, it remains challenge in tuning the corrugated morphology and controlling branching of these metallic filaments. The periodicity on metallic filaments can be controlled by applying external electric pulses, referring to the method in spontaneous formation of periodic nanostructured Cu [15]. Normally, templates can be applied in electrodeposition to achieve metallic structures with designed pattern, such as paralleled metallic wires [25–27]. With these methods, the propagation of surface waves along periodical and corrugated structures could be better controlled. They may be taken into applications in infrared region, such as sensors or detectors.

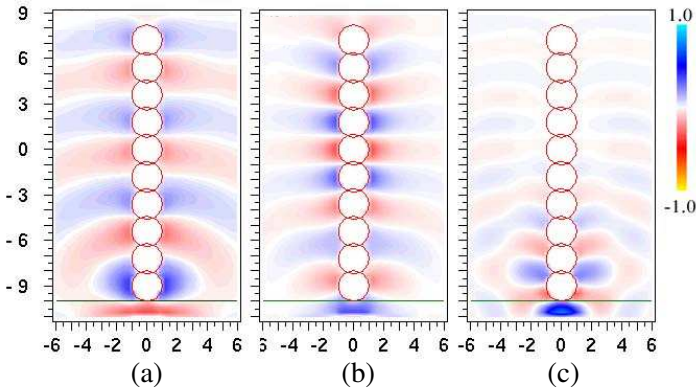


**Figure 4.** Electric field distribution on the cross section along silver spherical chain axis at different wave numbers. (a)  $1818\text{ cm}^{-1}$ , (b)  $2222\text{ cm}^{-1}$ , (c)  $3030\text{ cm}^{-1}$ . Electromagnetic waves are all incident from the bottom of silver spherical chains.

#### 4. CONCLUSION

Single-crystalline filaments with pearl-chain-like structures can be fabricated by electrodeposition without using any templates, surfactants, and additives. Transmittance enhancement through these silver filaments with pearl-chain-like structures can be identified within a certain frequency range of infrared. Excited surface waves may sustain on the surface of silver pearl chains, and electromagnetic waves can propagate along them. Based on the propagation profile on silver filaments, we suggest that these silver filaments with pearl-chain-like structures may have applications in Mid-IR transmission or detection.

#### ACKNOWLEDGMENT

This work is supported by NSFC (Grant No. 60071043 and 60532010) and the Doctor Station Foundation of the Ministry of Education of China (Grant No. 200806140007).

#### REFERENCES

1. Howes, M. J. and D. V. Morgan, *Microwave Devices: Device Circuit Interactions*, Wiley, New York, 1976.
2. Cook, N. P., *Microwave Principles and Systems*, Prentice-Hall, Englewood Cliffs, NJ, 1986.
3. Chedid, M., I. Belov, and P. Leisner, "Electromagnetic coupling to a wearable application based on coaxial cable architecture," *Progress In Electromagnetics Research*, Vol. 56, 109–128, 2006.
4. Crozier, K. B., E. Togan, E. Simsek, et al., "Experimental measurement of the dispersion relations of the surface plasmon modes of metal nanoparticle chains," *Optics Express*, Vol. 15, 17482–17493, 2007.
5. Wei, Q.-H., K.-H. Su, S. Durant, et al., "Plasmon resonance of finite one-dimensional Au nanoparticle chains," *Nano Lett.*, Vol. 4, 1067–1071, 2004.
6. Maier, S. A., M. L. Brongersma, P. G. Kik, et al., "Observation of near-field coupling in metal nanoparticle chains using far-field polarization spectroscopy," *Phys. Rev. B*, Vol. 65, 193408, 2002.
7. Pendry, J. B., L. Martin-Moreno, and F. J. Garcia-Vidal, "Mimicking surface plasmons with structured surfaces," *Science*, Vol. 305, 847–848, 2004.
8. Maier, S. A., S. R. Andrews, L. Martín-Moreno, et al., "Terahertz surface plasmon-polariton propagation and focusing

- on periodically corrugated metal wires,” *Phys. Rev. Lett.*, Vol. 97, 176805, 2006.
9. Ji, Y. B., E. S. Lee, J. S. Jang, et al., “Enhancement of the detection of THz Sommerfeld wave using a conical wire waveguide,” *Optics Express*, Vol. 16, 271–278, 2008.
  10. Kong, F. M., K. Li, B. I. Wu, et al., “Propagation properties of the SPP modes in nanoscale narrow metallic gap, channel, and hole geometries,” *Progress In Electromagnetics Research*, Vol. 76, 449–466, 2007.
  11. Menachem, Z. and M. Mond, “Infrared wave propagation in a helical waveguide with inhomogeneous cross section and application,” *Progress In Electromagnetics Research*, Vol. 61, 159–192, 2006.
  12. Kumar, N. and S. P. Ojha, “Photonic crystals as infrared broadband reflectors with different angles of incidence: A comparative study,” *Progress In Electromagnetics Research*, Vol. 80, 431–445, 2008.
  13. Wang, M., S. Zhong, X.-B. Yin, et al., “Nanostructured copper filaments in electrochemical deposition,” *Phys. Rev. Lett.*, Vol. 86, 3827–3830, 2001.
  14. Zhong, S., Y. Wang, M. Wang, et al., “Formation of nanostructured copper filaments in electrochemical deposition,” *Phys. Rev. E*, Vol. 67, 061601, 2003.
  15. Wang, Y., Y. Cao, M. Wang, et al., “Spontaneous formation of periodic nanostructured film by electrodeposition: Experimental observations and modeling,” *Phys. Rev. E*, Vol. 69, 021607, 2004.
  16. Wu, Z., Y.-J. Bao, G.-W. Yu, et al., “Characterization of periodically nanostructured copper filaments self-organized by electrodeposition,” *J. Phys.: Condens. Matter*, Vol. 18, 5425–5434, 2006.
  17. Wu, Z., H.-M. Li, X. Xiong, et al., “Electrodeposition of single-crystalline silver pearl chains,” *Appl. Phys. Lett.*, Vol. 94, 041120, 2009.
  18. Doremus, R. H., B. W. Roberts, and D. Turnbull, *Growth and Perfection of Crystals*, Wiley-VCH, Weinheim, Germany, 1958.
  19. Ming, N. B., *The Physical Base of Crystal Growth*, Shanghai Science Technology Press, Shanghai, 1982.
  20. He, R., X. Qian, J. Yin, et al., “Formation of silver dendrites under microwave irradiation,” *Chem. Phys. Lett.*, Vol. 369, 454–458, 2003.
  21. Geddes, C. D., A. Parfenov, I. Grycznski, et al., “Fractal silver

- structures for metal-enhanced fluorescence: Applications for ultra-bright surface assays and lab-on-a-chip-based nanotechnologies,” *Journal of Fluorescence*, Vol. 13, 119–122, 2003.
22. Huang, H., Y. Fan, B.-I. Wu, et al., “Tunable TE/TM wave splitter using a gyrotropic slab,” *Progress In Electromagnetics Research*, Vol. 85, 367–380, 2008.
  23. Aliakbarian, H., A. Enayati, G. A. E. Vandenbosch, et al., “Novel low-cost end-wall microstrip-to-waveguide splitter transition,” *Progress In Electromagnetics Research*, Vol. 101, 75–96, 2010.
  24. Shi, Y. C., “A compact polarization beam splitter based on a multimode photonic crystal waveguide with an internal photonic crystal section,” *Progress In Electromagnetics Research*, Vol. 103, 393–401, 2010.
  25. Zhang, M., S. Lenhert, M. Wang, et al., “Regular arrays of copper wires formed by template-assisted electrodeposition,” *Adv. Mater.*, Vol. 16, 409–413, 2004.
  26. Zhang, B., Y.-Y. Weng, X.-P. Huang, et al., “Creating in-plane metallic-nanowire arrays by corner-mediated electrodeposition,” *Adv. Mater.*, Vol. 21, 1–5, 2009.
  27. Yang, X.-C., X. Zou, Y. Liu, et al., “Preparation and characteristics of large-area and high-filling Ag nanowire arrays in OPAA template,” *Materials Letters*, Vol. 64, 1451–1454, 2010.